

SUPPLEMENTARY FIGURES

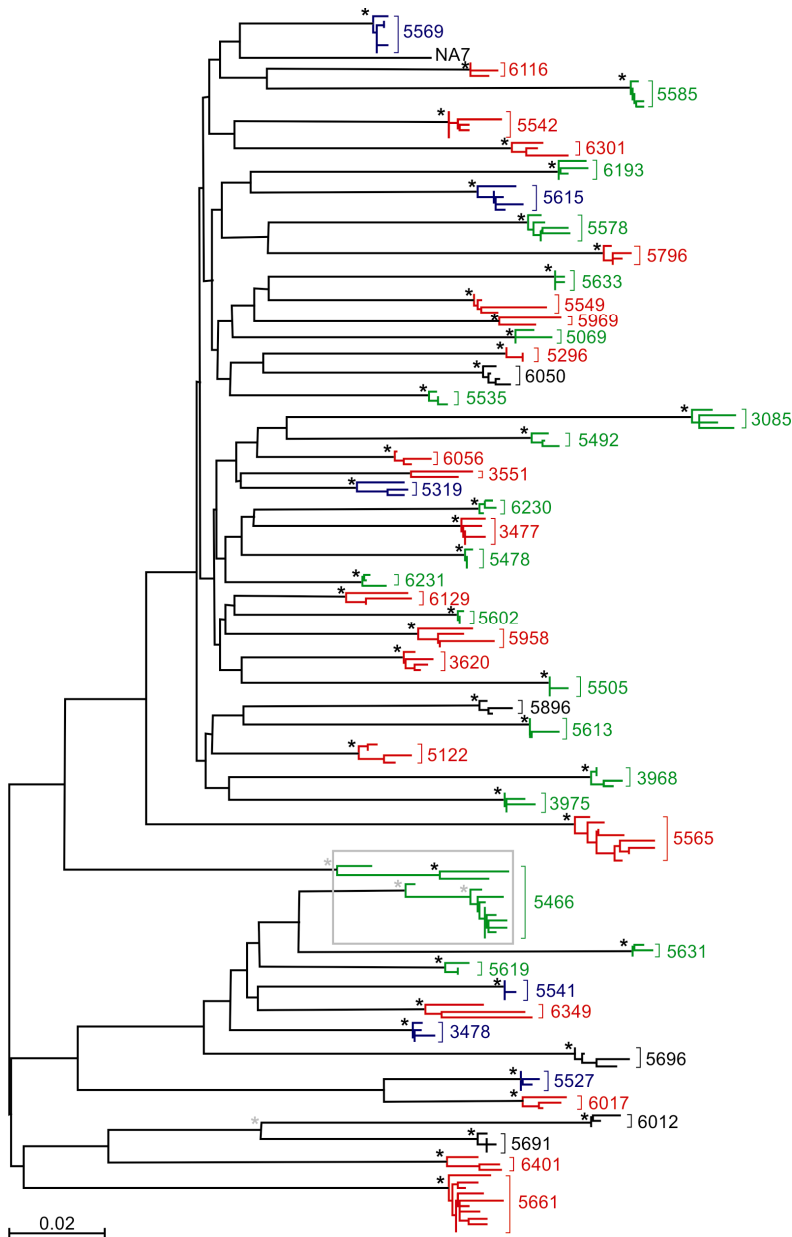


FIG. S1. Evolutionary relationships of primary HIV-1 Nef alleles. The amino acids of the newly amplified Nef alleles were aligned with NA7 (GenBank accession number DQ242535) using ClustalX (41) and amino acids were replaced by codons. Sites with a gap in any sequence were eliminated. The tree was constructed using the neighbor-joining method implemented in ClustalX using Kimura's correction and 1000 bootstrapped replicates. Black asterisks (*) on branches indicate 100% support for the cluster to the right. Grey asterisks indicate bootstrap support between 97% and 99%. Patient clusters are labeled according to their genotype and viral setpoint as defined in Fig. 1, with red indicating *-35CChi*, blue *-35CCLow*, green *-35TThi* and black *-35TTlow* subjects, respectively. Sequences from patient 5466 who was coinfecting with two divergent HIV-1 strains are boxed. Scale bar represents 0.02 substitutions per site.

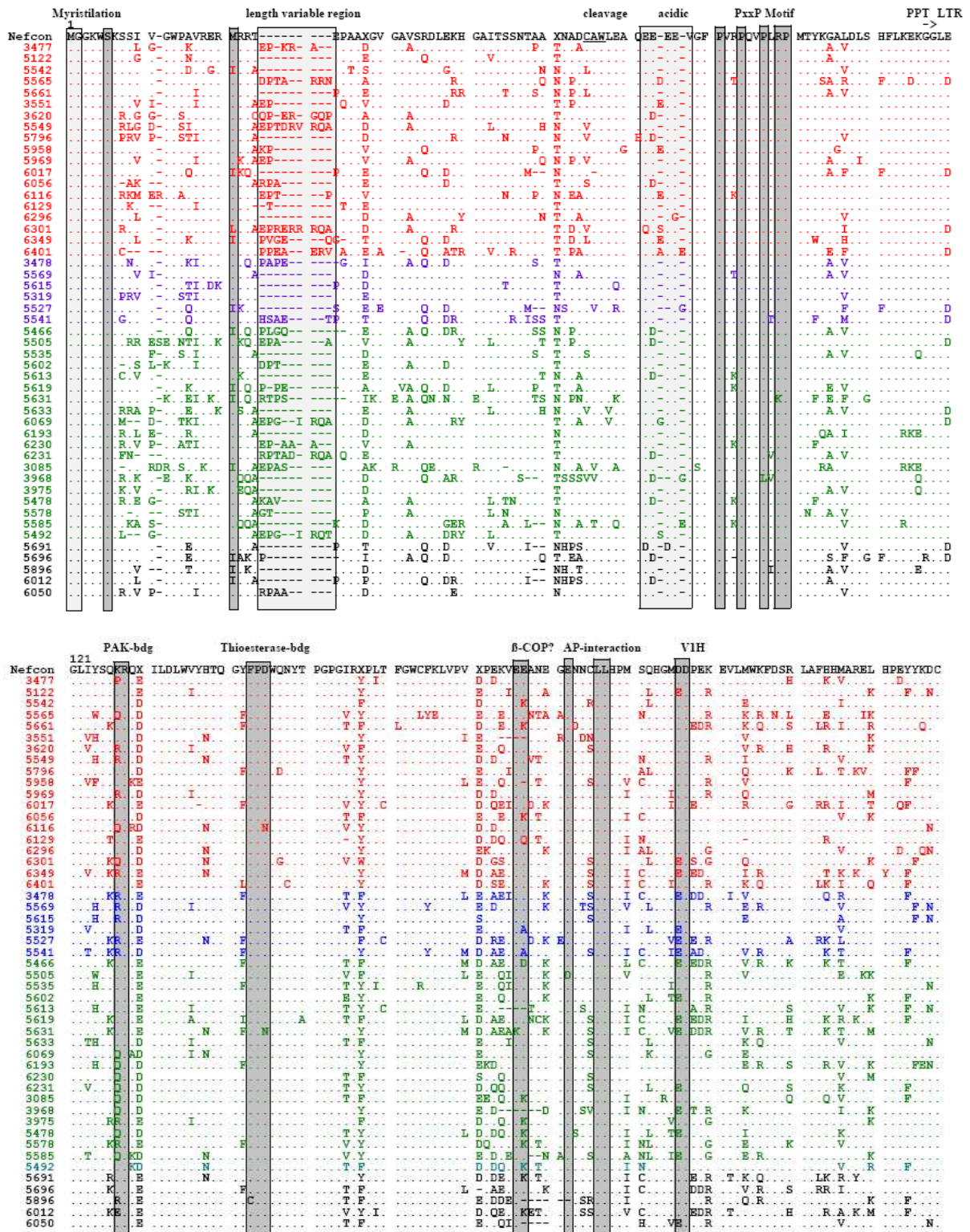


FIG. S2. Alignment of consensus HIV-1 Nef amino acid sequences. Newly derived Nef sequences are aligned with their overall consensus sequence, with dots indicating identity and dashes gaps introduced to optimize the alignment. Nef sequences are color coded as in Fig. 1, with red indicating *-35CChi*, blue *-35Cclow*, green *-35TThi* and black *-35Tllo* subjects, respectively. For patient 5466, only the predominant Nef sequence is shown. Some conserved sequence elements in Nef, the position of the polypurine tract (PPT), and the start of the 3' long terminal repeat (LTR) are indicated. bdg, binding; VIH, catalytic subunit of vacuolar ATPase.

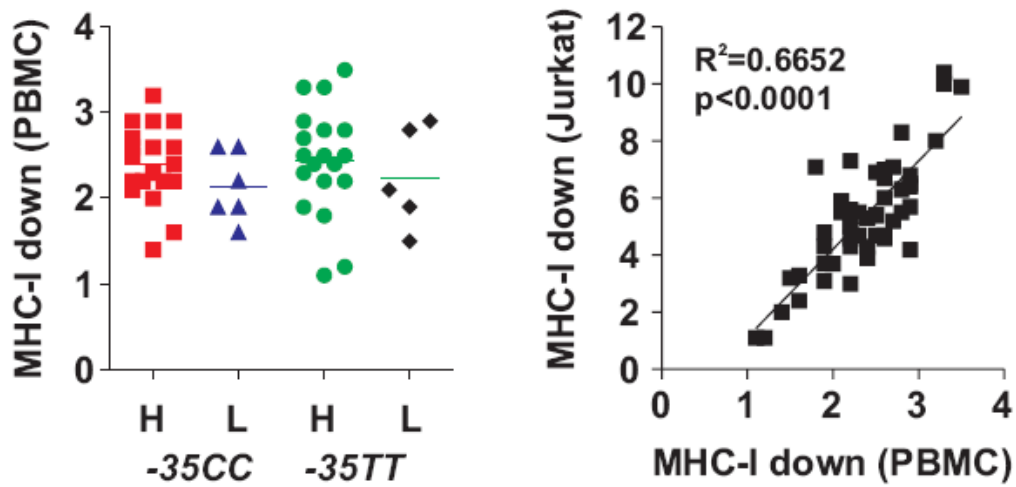


FIG. S3. Modulation of MHC-I by Nef in primary PBMCs. (Left) Quantitative assessment of Nef-mediated downmodulation of MHC-I on human PBMCs. Similar results were obtained using PBMC from a different donor. (Right) Correlation between the efficiency of Nef-mediated downmodulation of MHC-I in Jurkat T cells and PBMCs.

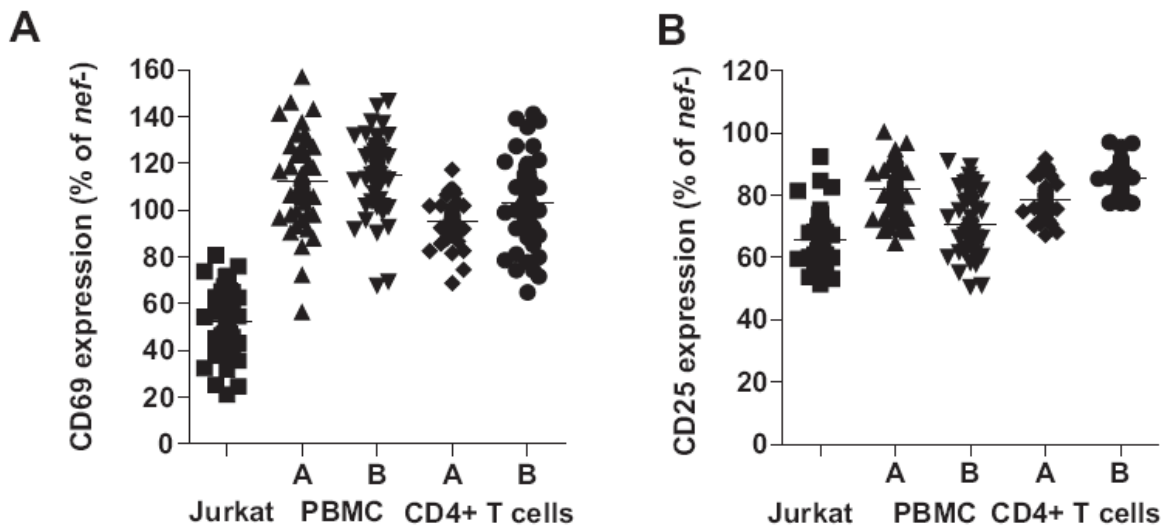


FIG. S4. Cell type dependent effect of Nef on early T cell activation. Levels of (A) CD69 and (B) CD25 expression by Jurkat cells, PBMCs and primary CD4⁺ T cells infected with HIV-1 IRES/eGFP constructs. The expression levels are given relative to those measured for the *nef* defective control HIV-1 construct which was set to 100%. PBMCs and CD4⁺ T cells were derived from two different donors (A and B).

TABLE S2. Functional activity of HIV-1 *nef* alleles from -35TT or -35CC individuals with high or low set-point viral loads.

Group	Receptor modulation ^a								T cell activation ^b			
	MHC-I	HLA-A	HLA-B	HLA-C	CD4	CD28	CXCR4	CD74	NF-AT	CD69	Infectivity ^c	Repl.(%) ^d
-35CC/sVLh (n=19)	5.1±0.3	3.7±0.3	3.7±0.3	1.7±0.1	3.8±0.2	1.5±0.1	1.6±0.1	5.0±0.4	124±12	95±3	8.0±0.7	133±12
-35CC/sVLI (n=6)	4.6±0.6	3.5±0.5	3.6±0.5	1.8±0.2	2.9±0.2	1.2±0.1	1.4±0.1	3.1±0.7	195±21	98±5	4.8±0.6	136±32
-35TT/sVLh (n=19)	6.0±0.6	4.2±0.5	4.2±0.5	2.0±0.2	3.7±0.3	1.6±0.1	1.5±0.1	5.6±0.6	174±12	101±3	6.4±0.5	170±13
-35TT/sVLI (n=5)	4.9±0.6	3.1±0.3	3.1±0.4	1.7±0.4	4.8±0.3	1.6±0.1	1.9±0.3	5.2±1.2	218±59	107±6	6.8±1.1	165±22

^a N-fold down-modulation of CD4, CD28, CD3, MHC-I, MHC-II and up-regulation of Ii surface expression levels were determined as described in the Materials and Methods. In all analyses at least 500 HIV-1-infected (GFP+) cells were analyzed. Shown are average values derived from three to five independent experiments (\pm SD).

^b Values were determined as described in the legend to Fig. 5.

^c Shown is the n-fold enhancement of viral infectivity compared to the *nef*-deleted HIV-1 NL4-3 control construct. Values represent the average of three measurements (\pm SD).

^d The efficiency of virus spread was determined in PBMC and is shown relative to the proviral HIV-1 NL4-3 Nef (*nef*+) construct (100%)